Out of Axis Movement of an AUV inside a Water Pipeline

M. Moonesun[*,a], A. Mahdian[b], Y.M. Korol[c] and A. Brazhko[d]

[*a] *National University of Shipbuilding Admiral Makarov (NUOS), Faculty of Ship Design, Ukraine.*
[b] *Malek University of Technology (MUT), Mechanical Engineering Department, Iran.*
[c] *National University of Shipbuilding Admiral Makarov* (NUOS), *Faculty of Ship Design, Ukraine.*
[d] *National University of Shipbuilding Admiral Makarov (NUOS), Faculty of Ship Design, Ukraine.*

Received 23 December 2014; Accepted 26 June 2016

Abstract: The research intends to evaluate the variation in the resistance and the lift of a torpedo shaped AUV brought about by the wall effect inside the pipe as it moves out of the axis inside a water pipeline. Movement of an AUV at the axis of a pipe causes minimum resistance and lift forces, but when the AUV moves at a position parallel with the axis of the pipe (out of axis of the pipe), the hydrodynamic forces especially the lift force changes. The AUV must be able to move a float inside the pipe and perform non-contact inspection. In water pipes having limited diameters, there is the wall effect. The added resistance and the lift have to be calculated accurately, which is a necessary requirement for the determination of the vehicle speed, power demand, control, range and duration of the operation. According to the findings of this paper, when moving at the center of pipe the ratio of AUV diameter to pipe diameter is equal to 12. This value can be considered for the determination of "the critical pipe diameter" which gives zero resistance. The results of this study can be applied for torpedo movement inside the torpedo tube. The analysis is performed by the Flow Vision (V.2.3) software based on the CFD method and solving the RANS equations.

Key world: AUV, pipeline, hydrodynamic, resistance, lift, wall effect.

حركة خارج المحور لمركبة مستقلة تحت الماء داخل أنابيب المياه

م. موونسن[أ,*] ، أ. ماهديان[ب] ، ي. م. كورول[ت] ، أ. برازهكو[ث]

الملخص: يعتزم هذا البحث تقييم التغيير في المقاومة والرفع لمركبة مستقلة تحت الماء AUV على شكل طوربيد داخل أنابيب المياه من تأثير الجدار داخل الأنبوب أثناء الحركة خارج المحور. الحركة للمركبة في محور الأنبوب تسبب مقاومة وقوة رفع أقل ولكن عندما تتحرك المركبة في وضع موازي لمحور الأنبوبة؛ تتغير القوة الهيدروديناميكية وخاصة قوة الرفع. المركبة المستقلة تحت الماء AUV يجب أن تكون قادرة على الحركة العائمة داخل الأنبوب لتؤدي الفحص بدون تلامس. ففي مواسير المياه ذات الأقطار المحدودة يظهر تأثير الجدار. ولتحديد سرعة المركبة، والقدرة المطلوبة، والتحكم، المدى وفترة التشغيل؛ لابد من حساب المقاومة المضافة والرفع بدقة لأن هذا يعتبر متطلب ضروري. ووفقاً لنتائج هذه المقالة؛ التحرك في مركز الأنبوب والنسبة بين قطر المركبة لقطر الأنبوب تساوي ١٢، هذه القيمة تستخدم لإيجاد القطر الحرج للماسورة وتكون قيمة المقاومة المضافة في هذه الحالة تساوي صفر. نتائج هذه الدراسة يمكن تطبيقها على حركة الطوربيد داخل ماسورة الطوربيد. أجريت التحاليل باستخدام برنامج رؤية التدفق (V.2.3) والذي يعتمد على طريقة CFD وحل معادلات RANS.

الكلمات المفتاحية: مركبة مستقلة تحت الماء، أنابيب المياه، الهيدروديناميكا، المقاومة، الرفع، تأثير الجدار.

* Corresponding author's email: m.moonesun@gmail.com

Nomenclature

a	Distance from pipe axis to AUV axis (m)
A_1	Section area of the model
A_2	Section area of water between model and pipe wall
AUV	Autonomous Underwater Vehicles
D	Maximum diameter of AUV (m)
d	Diameter of pipe (m)
e	Ratio of out of axis to the pipe radius (e=a/R)
IHSS	Iranian Hydrodynamic Series of Submarines
L	Overall length of hull (m)
l	Overall length of pipe (m)
P	Average Pressure of fluid between pipe and model (P_a)
Re	Reynolds number
R_f	Frictional resistance (N)
R_p	Pressure resistance (N)
R_t	Total resistance (N)
R_0	Total resistance in free stream (without pipe wall stream) (N)

* Other notations are referred.

1. Introduction

Water or petroleum pipelines are extended millions of kilometers all over the world. A severe breakdown of a pipeline may bring about large cost which might lead to pollution and accidents as well. Hence routine inspection and maintenance of the pipelines are necessary so that they can function trouble-free. Water supply is an essential public service and therefore inspection tasks cannot be compromised on continuity or quality. An inspection system must have the capacity to operate while the pipeline is in-service (Painumgal *et al.* 2013). Today several different pipeline inspection robots exist (Roman and Pellegrino 1993; Suzumori *et al.* 1998; Hirose *et al.* 1999; Muramatsu *et al.* 2000; Roh *et al.* 2001, Roh and Choi 2005; Moghaddam and Hadi 2005). The pipeline inspection robots presently are used by the contact with the walls for motion and positioning in the centre of the pipe (Okamoto *et al.* 1999). Figure 1 (Painumgal *et al.* 2013), shows the Autonomous Underwater Vehicle (AUV) inside a pipeline. This is a simple AUV with conical ends, but today modern AUVs are usually torpedo shaped. Discussion about submarine shape design is presented by Joubert (20040 and (Moonesun 2014). The aim of developing this inspection system is to enable non-destructive and non-disruptive inspection of water pipelines.

Recently torpedo shaped ocean going AUVs (Najjaran 2005) has been modified for inspecting large pipelines. The vehicles have been used to inspect very huge pipelines having a diameter of more than 2 meters. It is important for the pipeline internal inspection system to enter and leave the pipeline with the least disruption or damage to the pipe system. A great pipeline network means a great amount of pipeline network inspection. Hence, autonomous and free operation will be ideal for long distance inspection so as to avoid cable entanglement. Therefore, Autonomous Underwater Vehicles (AUV) are ideal tools for pipeline internal inspection (Painumgal *et al.* 2013).

2. Description of the Problem and Necessity

The flow field around a submarine inside a pipe or ducted space is different from that of a free stream. The proximity to the interior boundary of the hull induces wall effect on the fluid flow. In such cases, the boundary layer develops all over the circumference. The initial development of the boundary layer is similar to that over the flat plate. At some distance from the entrance, the boundary layers merge and further changes in velocity distribution become impossible. The velocity profile beyond this point remains unchanged. The distance up to this point is known as the entry length, which is about 0.04Re×d. The flow beyond this amount is said to be fully developed. The velocity profiles in the entry region and fully developed region are shown in Fig. 2. The flow is observed to be laminar until a Reynolds number value of about 2300. The Reynolds number is calculated based upon the basis of the diameter (ud/ν). In pipe flow, it is not a function of length. As long as the diameter is constant, the Reynolds number depends upon the velocity for a given flow.

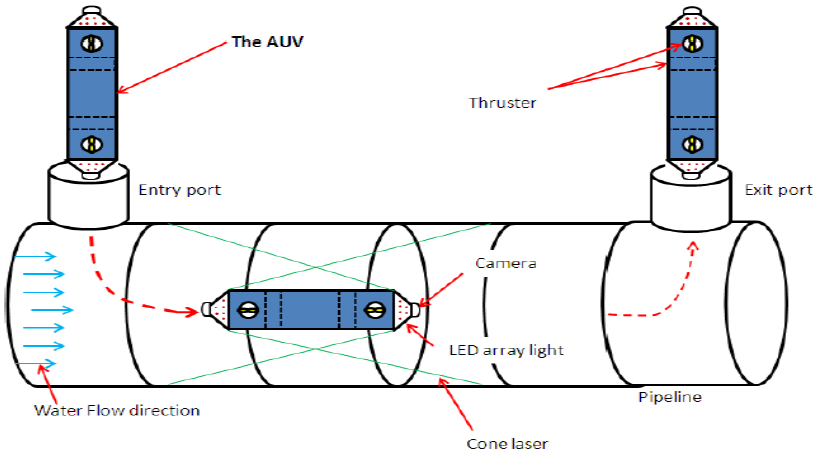

Figure 1. Schematic of pipeline inspection system and sample AUV (PICTAN) **(**Painumgal *et al.*2013).

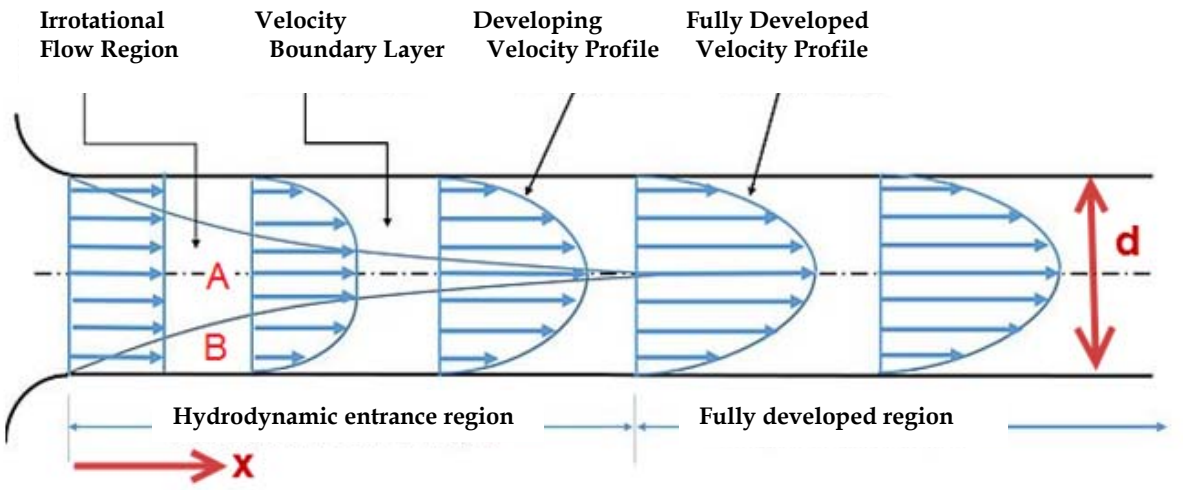

Figure 2. Boundary layer and velocity distribution inside a pipe in laminar flow.

Hence, the value of velocity determines the nature of flow in pipes for a given fluid. The value of the flow Reynolds number is decided by the diameter and the velocity. As shown in Fig. 2, region (A) is the non viscous flow not affected by the boundary layer, but region (B) is the boundary layer region. After some length, the boundary layers merge and the flow becomes fully developed. The entry length in turbulent flow is about 10 to 60 times the diameter. The velocity profile in the fully developed flow remains constant and is generally flatter compared to laminar flow for parabolic case. Now it seems clear that the flow through the pipe is different from that of a free stream. Should there be an initial flow stream inside the pipe, the entrance length must be regarded but if there is no flow speed and only the AUV moves, entrance length could be ignored. In the present research, only the AUV moves, and there is no initial fluid speed. When an AUV moves inside the pipe, it will experience the wall effects, especially in low diameter pipes. This causes an increase in resistance. The lower the pipe diameter, the higher the resistance. This added resistance should be calculated accurately, since it is a necessary requirement for the determination of vehicle speed, power demand, range and duration of operation. Another important parameter is out of axis movement of the AUV. Movement of an AUV parallel to the axis (at the axis) of a pipe, causes minimum resistance and minimum lift forces, but when AUV moves out of axis of the pipe, the hydrodynamic forces, especially the lift force changes.

3. Specifications of the Model and Pipe

For this research only the bare hull is to be studied. The base model considered here, is an axis-symmetric AUV similar to a torpedo, without any appendages. It helps to halve the CFD modeling of the body, which is a time saver. The total length is 2 meters, the diameter is 0.25 m, the wetted surface area is 1.35 m^2, the volume is 0.08 m^3 and the fineness ratio (L/D) is 8. The specifications of the model are presented in Fig. 3.

Dimensions of the model are constant, but the tube diameter (d) is different. For the present study, 10 pipe diameters are considered as follows; d/D=1.22, 1.41, 1.58, 1.73, 2, 3, 4, 10, 12 and 13 are shown in Fig. 4. The ratio of the water section area (A_2) to the section area of the model (A_1) is important. Some of the values of d/D are considered according to A_2/A_1. The values of d/D= 1.22, 1.41, 1.58 and 1.73 are respectively equivalent to A_2/A_1=0.5, 1, 1.5 and

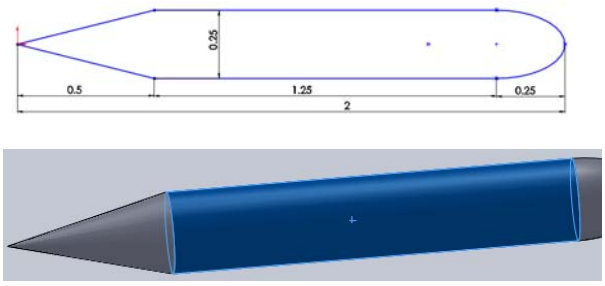

Figure 3. General configuration of the models.

2. Three different speeds are considered; 1, 3 and 10m/s. These speeds are considered so that all Reynolds number (ud/ν) values are more than 2300. This provides fully turbulent flow or transition zone inside the pipe. The usual speed of AUVs inside the tube is in the range of 1~3m/s but the speed of 10m/s is considered for such high speed vehicles as; the ejection of torpedo from the torpedo tube.

The out of axis movement of AUV, is evaluated for two values: d/D=4 and 12. The parameter "e", shows the ratio of out of axis to the radius of pipe (e=a/R). The parameter "a" is calculated from the axis of the pipe (Fig. 5). In the present study, four values of "e" are studied: e=0, 0.25, 0.5, 0.75.

4. CFD Method of Study

Governing Equations

- Viscosity or friction between fluid layers result in transfer of momentum from one fluid layer to another; this is a molecular level effect (due to rubbing of adjacent AUV molecules).
- Turbulent mixing resulting in additional apparent stress or Reynolds stresses (after Osburn Reynolds in 1880); this is a macroscopic effect due to bulk motion of fluid elements.

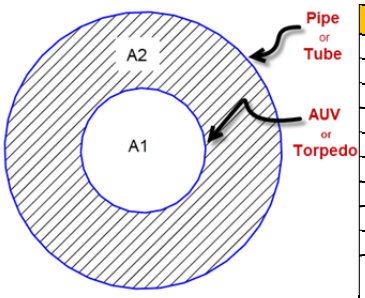

D (m)	d/D	A_2/A_1
0.304	1.22	0.5
0.36	1.41	1
0.394	1.58	1.5
0.432	1.73	2
0.5	2	2.9
0.75	3	7.8
1	4	14.7
2.5	10	97.1
3	12	140.3
3.25	13	164.8

$A_1=\pi D^2/4$, $A_2=\pi/4(d^2-D^2)$

Figure 4. Cross section area of AUV and pipe (hatched area: water between AUV and pipe).

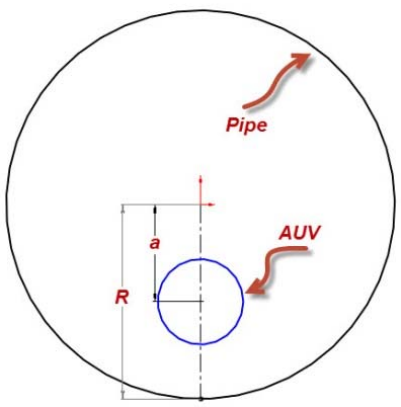

e = a/R
0
0.25
0.5
0.75

Figure 5. Out of axis movement of inside the pipe.

Momentum (Navier-Stokes) equation (3 components in Cartesian coordinates) in conservative form are as Eqn.1:

$$\rho\left[\frac{\partial u}{\partial t}+\frac{\partial(u^2)}{\partial x}+\frac{\partial(uv)}{\partial y}+\frac{\partial(uw)}{\partial z}\right]=-\frac{\partial p}{\partial x}+\frac{\partial}{\partial x}\left(\mu\frac{\partial u}{\partial x}\right)+\frac{\partial}{\partial y}\left(\mu\frac{\partial u}{\partial y}\right)+\frac{\partial}{\partial z}\left(\mu\frac{\partial u}{\partial z}\right)$$

$$\rho\left[\frac{\partial v}{\partial t}+\frac{\partial(v\,u)}{\partial x}+\frac{\partial(v^2)}{\partial y}+\frac{\partial(v\,w)}{\partial z}\right]=-\frac{\partial p}{\partial y}+\frac{\partial}{\partial x}\left(\mu\frac{\partial v}{\partial x}\right)+\frac{\partial}{\partial y}\left(\mu\frac{\partial v}{\partial y}\right)+\frac{\partial}{\partial z}\left(\mu\frac{\partial v}{\partial z}\right) \quad (1)$$

$$\rho\left[\frac{\partial w}{\partial t}+\frac{\partial(w\,u)}{\partial x}+\frac{\partial(w\,v)}{\partial y}+\frac{\partial(w^2)}{\partial z}\right]=-\frac{\partial p}{\partial z}+\frac{\partial}{\partial x}\left(\mu\frac{\partial w}{\partial x}\right)+\frac{\partial}{\partial y}\left(\mu\frac{\partial w}{\partial y}\right)+\frac{\partial}{\partial z}\left(\mu\frac{\partial w}{\partial z}\right)$$

Another form by using Einstein notation (sum each repeated index over i, j, and k) for Cartesian coordinates and the x-component where $(x_i , x_j , x_k) = (x , y , z)$ and $(u_i , u_j , u_k)= (u , v , w)$ are as Eqn. 2:

$$\rho\left[\frac{\partial(u_i)}{\partial t}+\frac{\partial(u_j u_i)}{\partial x_j}\right]=-\frac{\partial p}{\partial x_i}+\frac{\partial}{\partial x_j}\left(\mu\frac{\partial u_i}{\partial x_j}\right) \quad (2)$$

In terms of shear stress by using:

$$\tau_{ij}\,\mu\left(\partial u_i/\partial x_j+\partial u_j/\partial x_i\right),\text{ or mean strain rate,}$$

$S_{ij} = {}^{\tau_{ij}}/_{(2\mu)}$, the equation is reformed to Eqn. 3:

$$\rho\left[\frac{\partial(u_i)}{\partial t}+\frac{\partial(u_j u_i)}{\partial x_j}\right]\frac{\partial p}{\partial x_i}+\frac{\partial \tau_{ji}}{\partial x_j} \quad \text{or} \quad (3)$$

$$\rho\left[\frac{\partial(u_i)}{\partial t}+\frac{\partial(u_j u_i)}{\partial x_j}\right]=-\frac{\partial p}{\partial x_i}+\frac{\partial}{\partial x_j}(2\mu S_{ji})$$

Mean and fluctuating velocities and pressure can be represented as:

$$u_i(x,y,z,t)=\bar{u}_i(x,y,z)+u'_i(x,y,z,t) \text{ and } p(x,y,z,t)=\bar{p}(x,y,z)+p'(x,y,z,t).$$

Mean velocity is defined as:

$$\bar{u}=\frac{1}{T}\int_0^T u_t dt$$

Substitute in mean and fluctuating variables and expand to get the form of Eqn. 4:

$$\begin{aligned}\rho\left\{\frac{\partial(\bar{u}_i+u'_i)}{\partial t}+\frac{\partial\left[(\bar{u}_j+u'_j).(\bar{u}_i+u'_i)\right]}{\partial x_j}\right\} &= -\frac{\partial(\bar{p}+p')}{\partial x_i}\\ &+\frac{\partial}{\partial x_j}\left[\mu\frac{\partial(\bar{u}_i+u'_i)}{\partial x_j}\right]\\ \rho\left[\frac{\partial\bar{u}_i}{\partial t}+\frac{\partial(u'_i)}{\partial t}+\frac{\partial(\bar{u}_j\bar{u}_i)}{\partial x_j}+\frac{\partial(\bar{u}_j u'_i)}{\partial x_j}\right.&\\ \left.+\frac{\partial(\bar{u}_i u'_j)}{\partial x_j}+\frac{\partial(u'_j u'_i)}{\partial x_j}\right] &= -\frac{\partial\bar{p}}{\partial x_i}-\frac{\partial p'}{\partial x_i}\\ &+\frac{\partial}{\partial x_j}\left[\mu\frac{\partial\bar{u}_i}{\partial x_j}+\frac{\partial u'_i}{\partial x_j}\right]\end{aligned} \quad (4)$$

$$\bar{\bar{u}}_i=\bar{u}_i \quad \overline{\bar{u}_i+u'_i}$$
$$=\bar{u}_i+\overline{u'}_i=\bar{u}_i \quad \overline{\bar{u}_i.u'_i}=\bar{u}_i.\overline{u'}_j=0$$
$$\overline{\frac{\partial\bar{u}_i}{\partial x_j}}=\frac{\partial\bar{u}_i}{\partial x_j} \quad \overline{\bar{u}_i^2}=\bar{u}_i^2 \quad \overline{u'_i u'_j}<0$$
$$\frac{\partial u}{\partial t}\frac{\partial}{\partial x}(u^2)=\frac{\partial}{\partial x}[(\bar{u}+u')^2]=\frac{\partial}{\partial x}(\bar{u}^2+2\bar{u}u'+u'^2)$$

Many terms cancel to give Reynolds averaged Navier Stokes (RANS) equations as Eqn. 5:

$$\rho\left[\frac{\partial\bar{u}_i}{\partial t}+\frac{\partial(\bar{u}_j\bar{u}_i)}{\partial x_j}\right]=-\frac{\partial\bar{p}}{\partial x_i}+\frac{\partial}{\partial x_j}\left[\mu\left(\frac{\partial\bar{u}_i}{\partial x_j}\right)-\rho\overline{u'_j u'_i}\right] \quad (5)$$

$$\rho\left[\frac{\partial\bar{u}_i}{\partial t}+\frac{\partial(\bar{u}_j\bar{u}_i)}{\partial x_j}\right]=-\frac{\partial\bar{p}}{\partial x_i}+\frac{\partial}{\partial x_j}(2\,\mu\,\bar{S}_{ji}-\rho\overline{u'_j u'_i})$$

The term $(-\rho\overline{u'_i u'_j})$ is named Reynolds stresses. Reynolds stresses are positive because the velocity fluctuations are correlated through conservation of mass such that $\overline{u'_i u'_j}<0$. Reynolds stresses include 9 elements (only 6 independent) due to $\tau'_{ij}=\tau'_{ji}=-\rho\overline{u'_i u'_j}$ (where i = j for normal stress) as Eqn. 6:

$$\overline{u'_i u'_j}=\begin{bmatrix}\overline{u'^2} & \overline{u'v'} & \overline{u'w'}\\ \overline{v'u'} & \overline{v'^2} & \overline{v'w'}\\ \overline{w'u'} & \overline{w'v'} & \overline{w'^2}\end{bmatrix} \quad (6)$$

There are 7 unknowns (6 unknowns for velocities and one for pressure) but 4 equations (3 Navier Stokes and 1 continuity). Therefore there 3 transfer equations such as turbulent models such as k-ε. The eddy viscosity is also commonly called the turbulent viscosity and it is normally written as μ_t. Turbulent viscosity is defined based on Reynolds stress as: $\tau_t=-\rho\overline{u'v'}=\mu_t\frac{\partial u}{\partial y}$.

Therefore $\tau=\tau_o+\tau_t=(\mu_o+\mu_t)\frac{\partial u}{\partial y}$ and $\mu=\mu_o+\mu_t$, where μ_o is viscosity of laminar flow and μ_t is turbulent viscosity. For calculation of μ_t two kinds of turbulent models are used: 1) Eddy Viscosity Essential Equations such as: Boussinesq, Speziale, Launder and 2) Eddy Viscosity Models included 6 models: Standards k-ε, Extended k-ε, RNG k-ε, Anisotropic k-ε, Wilcox k-ω and SST k-ω. In this study, the equations employed are: Boussinesq and Standards k-ε Model. Boussinesq equation is stated as:

$$-\rho\overline{u'_i u'_j}=2\mu_t S_{ij}-\frac{2}{3}\rho k\delta_{ij} \quad (7)$$

Finally, for calculation of μ_t the model standards k-ε uses two parameters of k and ε:

$$k=\frac{1}{2}\overline{u'_i u'_i}\ ,\ \varepsilon=\left(\frac{\mu}{\rho}\right)\overline{u'_{i,j}\,u'_{i,j}}\ ,\ \mu_t=C_\mu\rho\frac{k^2}{\varepsilon} \quad (8)$$

All notations of these equations are represented by Sanieenezhad M (2003).

4.2 Condition "A"

First, the resistance of the AUV at the center of the pipe is analyzed. Under this condition the lift force is zero, due to symmetry. The analysis is performed by Flow Vision (V.2.3) software based on CFD method and solving the RANS equations. Generally, the validity of the results of this software have been verified using several experimental test cases. Nowadays the software is accepted as a practical and reliable tool in CFD activities. The present research utilizes finite volume method (FVM) in order to model the cases. A structured mesh with cubic (hexahedral) cell has been used to map the space around the AUV. Transition of laminar layer to the turbulent layer in the boundary layer, and the flow separation are very determining factors in calculating the resistance. The two significant parameters in CFD for modeling the boundary layer- are Y^+ and mesh numbers, which to be selected with great care. For modeling the boundary layer near solid surfaces, the first cell height was placed such that the Y^+ is kept in the range of 30~100. It must be clarified that to reach a fine cells near the wall, each mesh near the solid surface is divided into eight smaller meshes. It means that each dimension of hexahedral mesh is divided into two from the middle, and therefore, each mesh converts to eight smaller fine meshes. In order to select the proper quantity and dimensions of the cells, for one specific condition ($d/D=1.41$, $A_2/A_1=1$) and $v=3m/s$, seven different type of meshes were selected and the results of the resistance forces were compared. The results remained almost constant after 1.9 millions meshes, showing that the results are independent of meshing (Fig. 6). Finally all models the mesh numbers considered are more than 2.1 million.

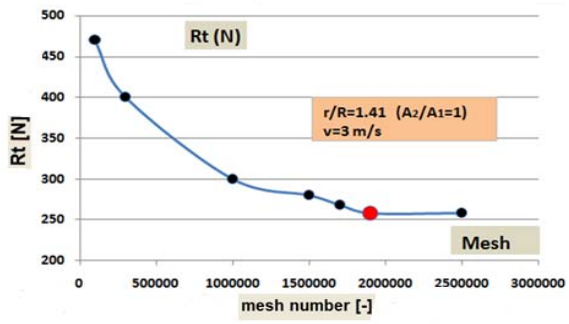

Figure 6. Mesh independency evaluations.

Due to the axis-symmetric shape and the axis-symmetry of the flow current, a quarter of the body and the domain are modeled. In the domain, there is an inlet (with uniform flow), a free outlet, a symmetry (in the two faces of the symmetric plane) and a wall (for the body of AUV and for the pipe interior boundary) (Fig. 7). In the present study it is supposed that the water inside the pipe remains calm having no speed, and only AUV moves. The turbulence model is K-ε are turbulent scale is considered 0.1m and y^+ 30~100. The considered flow is incompressible fluid (fresh water) at 20 degrees centigrade and velocities of 1, 3, 10m/s. Settings of the simulation are collated in Table 1.

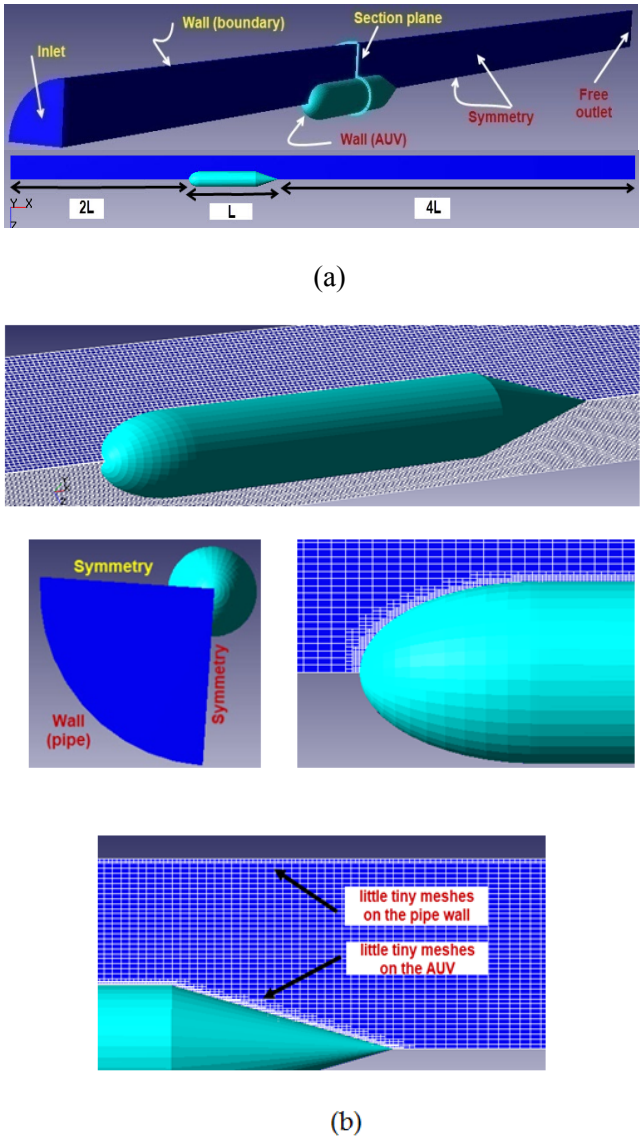

Figure 7. (a) Domain and general dimensions (b) Structured grid and very tiny cells near the wall for boundary layer modeling.

Table 1. Settings of the simulation (inside the pipe).

Elements	Boundary conditions	Descriptions	
Domain	Cylinder (quarterly)	Conditions	Fully submerged modeling (without free surface)- quarter and half modeling- domain with inlet, outlet, symmetry and wall- Without heat transfer.
		Dimensions	7L (distance before: 2L- distance after: 4L)*16R*16R
		Grid	structured grid- hexahedral cells- fine cell near wall- Meshes more than 2.1 millions.
		Settings	Iterations more that 700- Time step=0.01 s.
Fluid	-	Incompressible fluid (water)- Reynolds number, is different in each pipe- turbulent modeling: Standard k-ε- fresh water- tempreture:20 deg- ρ=999.841 kg/m^3.	
Object	Wall	Bare hull of AUV- value 30<y+<100 - roughness=0- no slip	
Input	Inlet	Velocity=1,3,10m/s- normal (along x)- in 1 face	
Output	Free outlet	Zero pressure- in 1 face	
Symmetry	Symmetry	In 2 faces	
Boundaries	Wall	For modeling the pipe wall- no slip condition	

The selection of the proper "time step" for each iteration, depends upon three parameters: 1) speed, 2) model length, and 3) mesh numbers along the main direction of the movement, as the transfer of network should be stopped on each section. For example, if v=1m/s, then the boundary layer will pass 2m the length of the body in 2 seconds.

The direction of velocity is along the axis, and we considered every 1 cm, one station of mesh, which means 200 longitudinal station along the body (not the whole domain). In order to stop the steam in each station, the time step is 2/200=0.01 seconds. On the other hand, the minimum time step is governed by:

$$\left(\frac{\text{body length/speed}}{\text{longitudinal station numbers on the body}}\right) \quad (9)$$

To select the suitable iteration number, it should be considered that boundary layer could travel the domain, from the beginning to the end. For example, if the full length of domain is taken to be 21m, and v=3m/s, 7 seconds is needed to traverse the total length, and if "time step is taken 0.01 s", a minimum number of 7÷0.01=700 iterations are needed. These conditions are collated in Table 1.

To analyze the pipe wall effect upon resistance, simulating the free stream, without the pipe and the wall effect is needed. The domain and the simulation are shown in Fig. 8. In the domain, there is an inlet (having uniform flow), free outlet, asymmetry (in the four faces of the box) and a wall (for the submarine body). The domain is a box with the dimensions of 12*2*2 m (or 6L*16R*16R).

4.3 Condition "B"

In this part, the out of axis position of AUV in the pipe is analyzed. Here, the quarter-model cannot be used, therefore, the half domain model is utilized (Fig. 9). Other conditions of the model remains same as that of "Condition A".

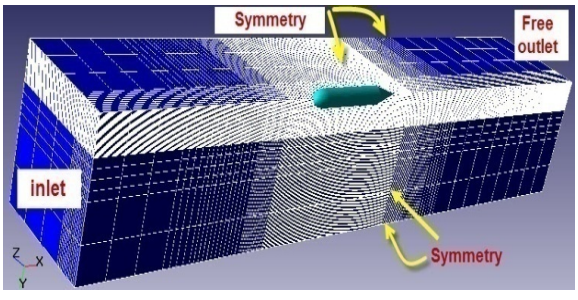

Figure 8. Free stream modeling (without pipe wall effects).

5. CFD Results and Analysis

5.1 Pressure Variation

In this case, there are two main factors: 1) pipe wall effect of the pipe and 2) change in flow speed. The pipe wall effect gives rise to boundary layer effects on the fluid, and a zero speed just on the wall. Fluid speed change appears due to the limited cross section area between the body and the pipe. The minor distance between the body and the pipe means minor cross section area (A_2). The flux of fluid is kept constant, therefore the fluid speed should be increased. An increase in the speed, according to Bernoulli's law, is equivalent to a decrease in pressure. For smaller values of A_2, the change in the fluid speed arising from the flux is more than the effect of boundary layer at the pipe wall. In next step, the variation in resistance and lift force of the model (AUV) is be discussed. The total resistance (R_t) is the summation of pressure resistance (R_p) and viscous resistance (R_f). Pressure resistance presents the effect of the shape of the body on the total resistance. On the other hand, this type of resistance is not dependent on the viscosity and boundary layer concepts. In our problem, the governing factor is pressure resistance, because it wholly depends upon the pressure distribution over the body. In each stage, the total and the pressure resistance are presented. The pressure variation under the condition of out of axis as per d/D=4 and speed of 3m/s for several values of "e" is shown in Fig. 10. As the figure shows, at e=0, the pressure distribution is uniform and axis symmetric. Hence, the lift force is expected to be zero. By getting out of axis, the fluid velocity at the top of the body decreases and then, the pressure increases. At the low end of the body, these variations are inverse: the velocity increases and the pressure decreases. Therefore, there are visible changes in the lift force.

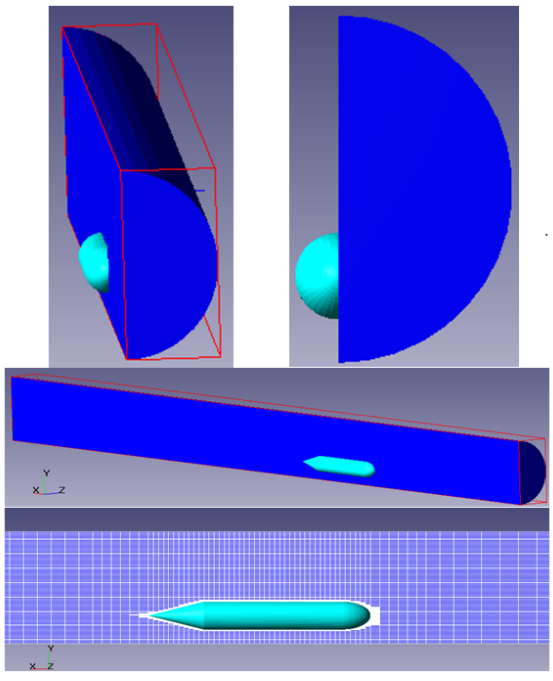

Figure 9. Out of axis model in flow vision.

5.2 Results of Analysis for Condition "A"

The total and pressure resistance of AUV for several different diameters of tubes are presented in Table 2. The results are presented for speeds of 1, 3, and 10 m/s. As is evident, at all speeds and for d/D <1.41 (or A_2/A_1<1), there is a jump in the resistance diagram. Therefore, it can be suggested that in all the pipes or torpedo tubes, d/D >1.41 (or A_2/A_1>1) should be considered. In the swim out of the self-prope-

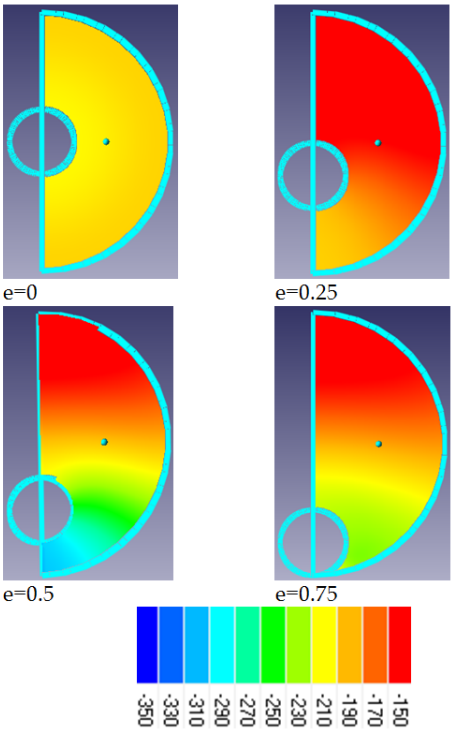

Figure 10. Pressure variation for several ratios of out of axis "e" for d/D=4 and v=3m/s.

lled system of the torpedoes in submarines, the torpedo diameter is 533 mm and the torpedo tube (launcher) is 640 mm, which eventuates measurements of A_1 = 0.223 m² and A_2 = 0.0985 m². For easier ejection of a torpedo from a tube, a minimum tube diameter of 750 mm is recommended, which results in $A_1 = A_2$. The main limitation for increasing the tube diameter is the architectural arrangement inside a submarine or a naval ship, and the volume of water required for filling the volume between the torpedo and the tube. This volume of water must be maintained at a high level inside the submarine tanks, but in pipelines, there is no such restriction. The diameter of the AUV can be designed according to the diameter of the pipe. The variation shows that, after d/D = 1.41, there is slight variation. Logically, by increasing the pipe diameter, there should be a decrease in resistance values.

At the speeds of 1m/s and 3m/s, the results after d/D=12 remain constant and is equal to results of large diameters. The values of "d/D=∞" is related to condition "B", which models the free stream condition. This means that after this limit, the added resistance and wall effect of pipe is negligible. This diameter is "the Critical Diameter". At the speed of 10m/s, the critical diameter occurs at d/D=13. Since there exists no high speeds in pipes, it can be concluded that d/D=12 is related to the critical diameter. The ratio of the pressure resistance to total resistance is shown in Fig. 11. As mentioned above, the pressure resistance has a unique role in determining total resistance. This diagram shows that in value of d/D<1.41, the pressure resistance is about 90 percent of total resistance. In large diameters, this value is about 45 percent. This means that the wall effect of the pipe, has brought about twice as much pressure resistance. By increasing the diameter, the portion of the pressure resistance will be decreased gradually.

To interpolate the other values of d/D, the best curve fitted to these points is provided by Curve expert software and least mean square (LMS) method. The extracted formula is:

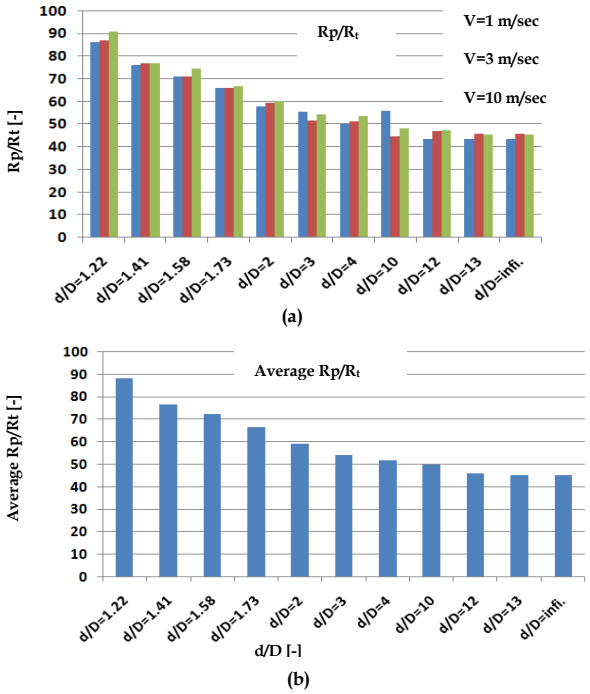

Figure 11. Ratio of pressure resistance to total resistance: (a) at different velocities and (b) average value.

Table 2. Values of total resistance and pressure resistance in several d/D at e=0.

d/D	v=1 m/s		v=3 m/s		v=10 m/s	
	R_t (N)	R_p (N)	R_t (N)	R_p (N)	R_t (N)	R_p (N)
1.22	145.2	125.2	1110.8	963.6	12820	11624
1.41	34.8	26.4	258	198	2392	1838
1.58	22	15.6	160.8	114	1099.2	820
1.73	15.2	10	115.2	76	1075.2	715.6
2	10.4	6	78.4	46.4	741.2	445.6
3	7.2	4	50.4	26	490	266
4	6	3	46	23.6	444	238
10	6	3.36	37.6	16.8	358	172
12	4.6	2	36.8	17.2	352.4	166
13	4.6	2	36.6	16.8	348	158
Infinity	4.6	2	36.6	16.8	348	158

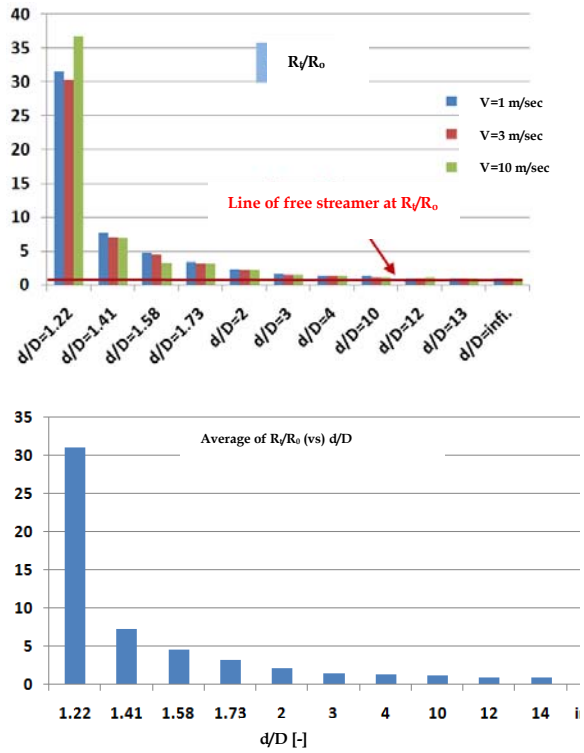

Figure 12: Ratio of total resistance to free stream resistance.

$$\frac{R_p}{R_T} = \frac{43.5\ (d/D)}{-0.61 + (d/D)} \qquad (10)$$

For a better understanding of pipe wall effect on the resistance, the ratio of total resistance to free stream resistance is presented in Fig. 12. The amount of R_t/R_0=1 shows that the wall effect is negligible, and the free stream condition is established.

To interpolate the other values of d/D, according to the best fitted curve by least mean square (LMS) method, the related formula is as follows:

$$\frac{R_T}{R_0} = \frac{1.01}{1 - 2.06e^{-0.62\left(\frac{d}{D}\right)}} \qquad (11)$$

As mentioned above, the ratio of d/D=12 can be regarded as critical diameter, neglecting the added resistance, and the pipe wall effect.

5.3 Results of Analysis for Condition "B"

The off-axis movement effect is studied for two values of d/D=4 and 12, at speeds of 1,3,10 m/s for values of e=0, 0.25 and 0.75. The compared results are shown in Figs. 13 and 14. For d/D=4, the variation of resistance at low and medium speeds are very little, but for e=0.75, it is considerable, as the body gets very

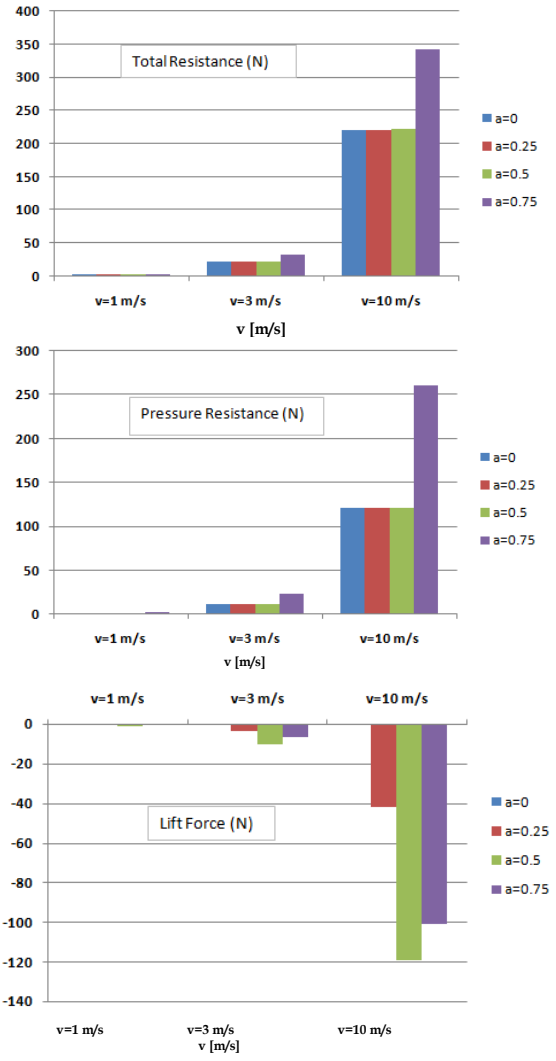

Figure 13. Diagram of hydrodynamic forces for d/D=4 at different velocities.

close to the pipe wall. The changes in the lift force is very stiff owing to the asymmetric distribution of pressure, above and beneath the body. For every step of "e", approximately 300 percent of increase is found, except at "e=0.75", which is different, because at this position, because the body becomes tangent to the pipe wall. This results in changes in the pressure domain.

As was shown earlier, at d/D=12, a free stream at the center of the axis can be represented, but by getting out of the center of the pipe, the free stream becomes in valid. As before, the variation in resistance all speeds and all values of "e" is negligible. The changes in the lift force is very stiff too. For every step of "e", found approximately 3-10 times increase in the lift force is observed.

It can be concluded that the out-of-axis movement has little effect on the resistance, because the principal factor is the pressure

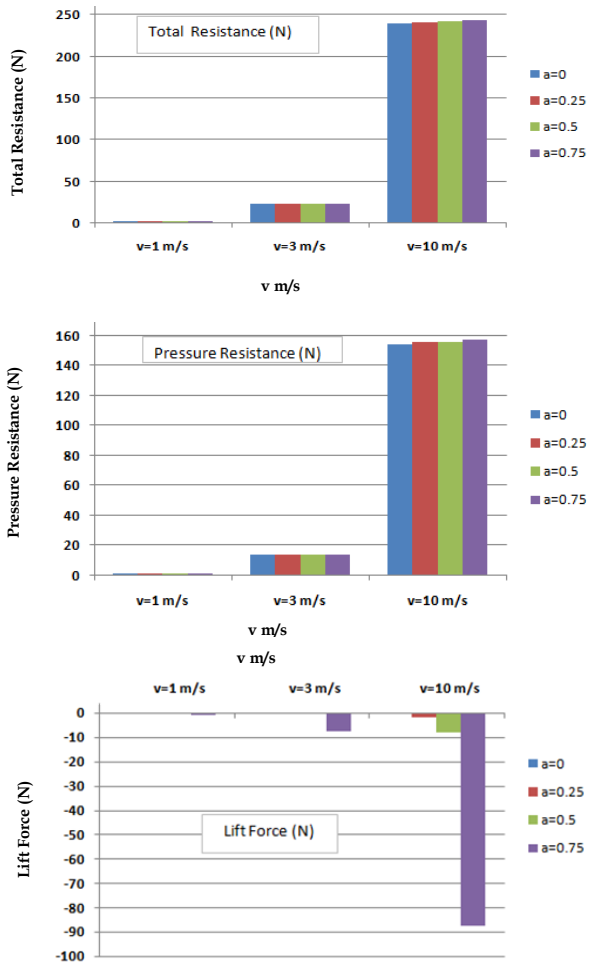

Figure 14. Diagram of hydrodynamic forces for d/D=12.

resistance. The pressure resistance is a function of fluid velocity around the body, which is the function of the flux. By changing the location of AUV inside the pipe, the fluid flux remains constant. Therefore, the changes in the pressure resistance and subsequently the total resistance is insignificant. The out-of-axis movement imposes a stiff variation in the lift force of the body. It is imperative neutralize this negative lift force in order to prevent hitting to the wall and the consequent damage. For this purpose, the hydroplanes of the AUV should be designed in such a way to produce inverse lift to neutralize the body lift force. That is, the hydroplanes should be designed to be able to produce such a big lift force. It is vital to keep the equilibrium and stability of the AUV while operating inside a pipe.

6. Conclusion

In conclusion, as regards to the added resistance of an AUV moving inside a pipe, arising from the wall effect, the followings can be suggested:

1- The ratio of d/D=12 can be regarded for the determination of "the critical pipe diameter" with added resistance zero.
2- The ratio of d/D<1.41 (or $A_2/A_1<1$) causes a stiff increase along with the resistance. Therefore, the values lower than this ratio are not recommended.
3- In the swim out launching system, for 533mm torpedoes, the minimum tube diameter of 750mm is recommended.
4- Pressure resistance has a crucial role in the total resistance of about 45~90 percent.
5- If there is an initial water speed inside the tube, the entrance length and the developed boundary layer has to be taken into account.
6- The fully developed condition of the stream, after the entrance length, provides about 5 percent decrease in the total resistance and a 10~20 percent decrease in the pressure resistance.
7- Out-of-axis movement of the AUV inside a pipe causes some change in resistance force.
8- Out-of-axis movement of the AUV inside a pipe imposes a stiff increase in lift force. Hydroplanes of AUV should be able to neutralize this body lift force.

References

Hirose S, Ohno H, Mitsui T, Suyama K (1999), A direct pneumatic stepping motor for robots: Design of Inpipe Inspection Vehicles for ø25,ø50,ø150 pipes. *IEEE International Conference on Robotics and Automation*. 2309-2314.

Joubert PN (2004), Some aspects of submarine design: part 1: Hydrodynamics, Australian Department of Defense.

Joubert PN (2004), Some aspects of submarine design: part 2: Shape of a Submarine 2026, Australian Department of Defense.

Kormilitsin YN, Khalizev OA (2001), Theory of submarine design. Saint Petersburg State Maritime Technical University, Russia 185-221.

Moghaddam M, Hadi A (2005), Control and guidance of a pipe inspection crawler (PIC), *22nd International Sysnposium on Automation and Robotics in Construction* 1-5.

Moonesun M, Javadi M, Charmdooz P, Korol UM (2013), Evaluation of submarine model test in towing tank and comparison with CFD and experimental formulas for fully submerged resistance. *Indian Journal of Geo-Marine Science* 42(8): 1049-1056.

Moonesun M (2014), Introduction of Iranian hydrodynamic series of submarines (IHSS). *J. of Taiwan Society of Naval Architecture and Marine Engineering* 33(3): 155-162.

Moonesun M, Mikhailovich KY, Tahvildarzade D, Javadi M (2014), Practical scaling method for underwater hydrodynamic model test of submarine. *J. of the Korean Society of Marine Engineering* Vol. 38(10): 850~857.

Muramatsu M, Namiki N, Koyama R, Suga Y (2000), Autonomous mobile robot in pipe for piping operations. *IEEE International Conference on Intelligent Robots and Systems* 2166-2171.

Najjaran H (2005), IRC creating an underwater robotic vehicle to inspect in service water mains. *Construction Innovation* 10(2): 11.

Okamoto J, Adamowskia JC, Tsuzukia M, Buiochia F, Camerinib CS (1999), Autonomous system for oil pipelines inspection. *Mechatronics.* Elsevier 731-743(13).

Painumgal U, Thornton B, Tamaki U, Nose Y (2013), Positioning and Control of an AUV inside a water pipeline for non-contact in-service inspection. www.mtsjournal.org / Papers / PDFs/130503-241.pdf,

Roh SG, Ryew SM, Yang JH, Choi HR (2001), Actively steerable in-pipe inspection robots for underground urban gas pipelines. *IEEE International Conference on Robotics and Automation* 1: 761-766.

Roh SG, Choi HR (2005), Differential-drive in-pipe robot for moving inside urban gas pipelines. *IEEE Transactions on Robotics and Automation*. 21(1): 1-17.

Roman H, Pellegrino BA (1993), Pipe line crawling inspections: An Overview. *IEEE Transactions on Energy Conversion* 8(3):

Sanieenezhad M (2003), An introduction to turbulent flow and turbulence modeling. *CFD Group publication* Iran.

Seif MS (2012), Fluid Mechanics. *Fadak publication*, Iran.

Suzumori K, Hori K, Miyagawa T (1998), A direct pneumatic stepping motor for robots: designs for pipe inspection Microrobots and for Human Care Robots. *IEEE International Conference on Robotics and Automation* 3047-3052.